Paving the way to hybrid helicopters

Prepared by - Pascal Chretien M.E.
emd3@generalmail.net

Abstract:

This paper describes the world's first 100% battery powered, manned helicopter. This challenging exercise provided a wealth of data on electrical propulsion. Although less than practical, the purpose of building this machine was to show that it can be done and to provide a springboard into future hybrid research. As battery capacity increases, the use of such hybrid designs expands into real civil and military roles.

Recent OGE free flights between July and August 2011 have demonstrated the impressive behavior of both power train and battery system for durations of up to 6 minutes, at discharge currents ranging from 480 to 560 Amps. The next logical step is to fly higher and longer (10 minutes). To date the craft has accumulated 99.5 minutes of flying time, over 29 flights.

The most cost-effective way to "recycle" this machine is to convert it into a hybrid UAV/optionally manned vehicle, by integrating an autopilot that would enable autonomous flights, or interpreted flight control system in a manned configuration. Reliable light 3 axis UAV boards are now available and only two small size servos (roll and pitch) will be required.

In its purely unmanned configuration, range extension will be achieved through an onboard fuel cell, or an internal combustion based generator that can be shut down on demand, offering extremely low infrared and acoustic signature, desirable for specific stealth mission profiles.

The end goal of this demonstrator is to pave the way to a hybrid helicopter, where gears, clutches, and shafts will all disappear. Instead, copper, batteries and an electromagnetic transmission will be used, in a highly redundant and flexible way. Key advantages of this configuration range from preventing autorotation through the use of sufficient onboard batteries enabling powered landing in case of generator failure, to significant power reserve at takeoff, with a drive train's weight no heavier than that of a conventional architecture.

Several patents and applications, covering amongst other things the architecture of a new electromagnetic transmission, the details of such a transmission, new battery pack architecture and others features, are contributing to the development of a new class of rotary wing machines offering unprecedented levels of safety and resilience to ballistic impact, at low running costs.

The suggested areas for immediate research are improved battery pack architecture design, power generation, and distributed electromagnetic transmission.

Trying to remain at high level, the following chapters will summarize some of the unconventional design features of the demonstrator, and in addition investigate the advantages offered by hybrid architectures applied to helicopters.

Demonstrator's design features:

Right from start, calculations showed that radically lightweight construction was necessary to efficiently utilize the limited power available,

With a consumption of 8 to 10 % of total hover power, a conventional tail rotor was not welcome (ref 12, 25). Side by side, intermeshing, propeller arrays, and coaxial configurations were all studied (ref 4). It was found that coaxial twin rotor would lead to smaller and lighter airframe, although not being as good as a side by side configuration as far as power requirement was concerned. Yet, for a thrust coefficient of 0.15, a coaxial helicopter offers an efficiency ratio of 0.8, as opposed to 0.7 for a conventional single rotor helicopter (ref 12). Asymmetrical 8H12 airfoils were eventually used, although symmetrical NACA 0012 airfoils were initially tested. FLUENT CFD showed that unequal rotor diameters were appropriate, for power optimization. Vertical rotor spacing to rotor diameter ratio of 0.13 was found to be optimal.

Conventional cyclic and flight controls were replaced by a weight shifting system, resulting in significant weight savings. However, this arrangement required flying with reversed roll and pitch controls, and a mechanical flight simulator was subsequently developed. Free flight stability analysis was conducted under MSC ADAMS (ref 25).

An energy absorbing composite landing gear was designed to withstand a 2 m drop and protect the 58 Kg of Li-ion polymer batteries located under the pilot's seat (ref 22, 26). For the pilot's safety, motors were positioned in such way that in case of crash they would tilt the rotor disks backwards. Spectra and Dyneema lines were extensively used for safety and structural reinforcement. Due to cost and time constraints, the airframe was made of welded 7020 Aluminum tubing. Although a few kilograms heavier than a composite airframe, this could be produced in days while still possessing fair and predictable crash worthiness.

Two separate methods were applied to ascertain power requirements in hover, and in flight: An analytical method, ran on MATLAB based on relations derived from flight tests and technical reports (Ref 3, 10, 14, 15, 19), where the coaxial system *for a given H/D ratio* (rotor spacing / rotor diameter) is reduced to a single equivalent rotor with the total number of blades and an *equivalent* diameter thereafter analyzed as a conventional rotor; and by 3D CFD analysis, using FLUENT (Figure 1).

The convergence of both methods validated power requirement estimation.

Early test flights revealed that both methods were overestimating the actual power by about 6 to 7 %, once reduced to standard conditions.

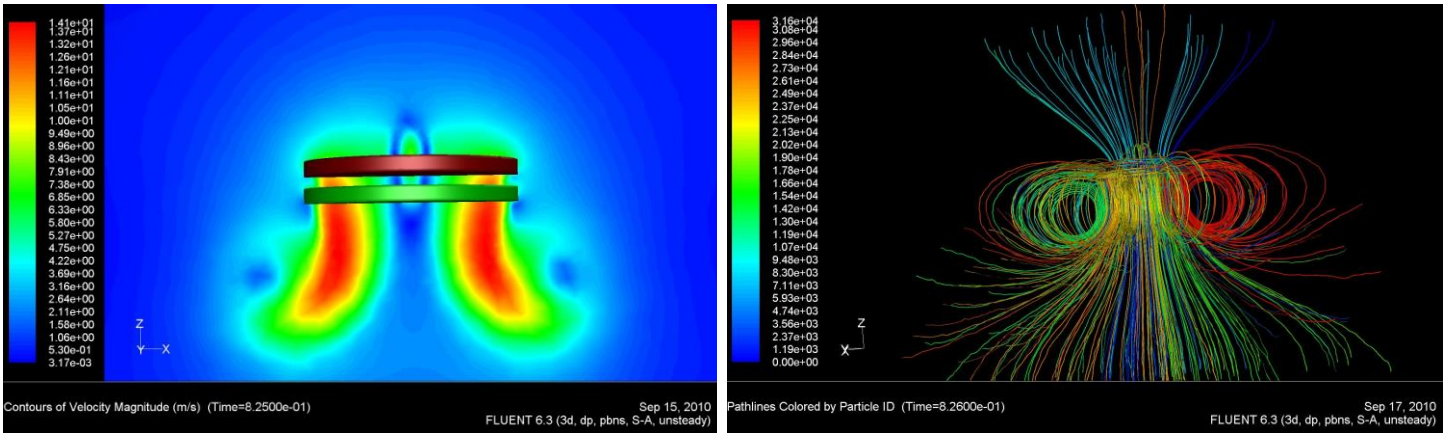

Figure 1:
Out of ground effect CFD Analysis of rotors showing contours of velocity on the left, and colored path lines on the right.

A somewhat unorthodox rotor system is used because given a fixed pitch system, rotor inertia is the enemy of power response; consequently, the blades had to be made as light as possible. An extruded multi cell structure (Figure 2) keeps the blade's weight down to 1.9 kg, yet offers outstanding torsional stiffness. Although not being optimum as far as fatigue is concerned, 6063 T6 alloy is an acceptable solution considering the short service life of our demonstrator; additionally, 6063 alloys exhibit relatively slow crack propagation. Daily blade inspection was part of the flight program.

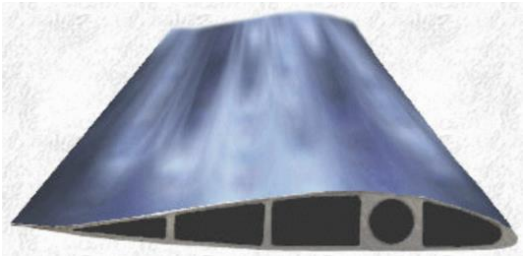

Figure 2: Multi cells blade

Leading edge balancing rods that usually bring the CG next to the center of lift, at ≈ 25% chord length were not used. The retention plates are located at 25% chord length, and the whole blade is pivoted forward by the lag link, at such an angle that mid span (0.5R) CG projected at the hub level is located at 25% chord (Figure 3). Some disadvantages of this solution are the resulting twisting moment, and subsequent risks of flutter. However, the short blades (2.1 m & 2 m for top and bottom rotor, respectively) are very stiff in torsion, and analysis suggested that flutter was not a concern.

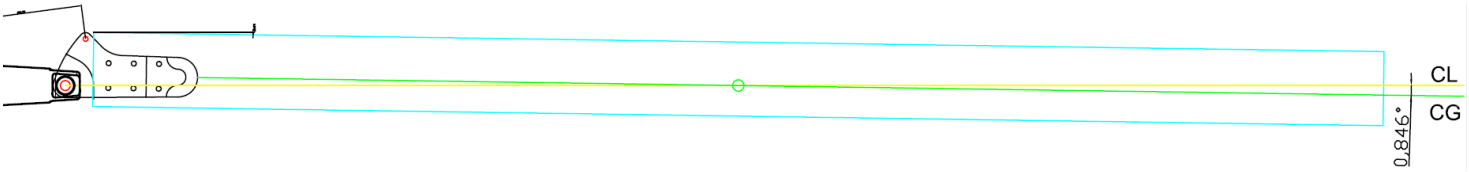

Figure 3: Blade lag setting.

Hysol 9466 compound was used to bond the retention plates onto the airfoil to spread the stresses out, as blade skin is only 1.1 mm thick and fasteners lead to unacceptably high localized stresses. Cell spaces directly located under the retention plates were filled with a low shrinkage epoxy based resin to achieve compressive strength and prevent high localized wedging stresses imparted by the outer end of the retention plates (due to blade root deflection, subsequent to variable coning angles). The following Finite Element Analysis (FEA) depicts the situation (Figure 4):

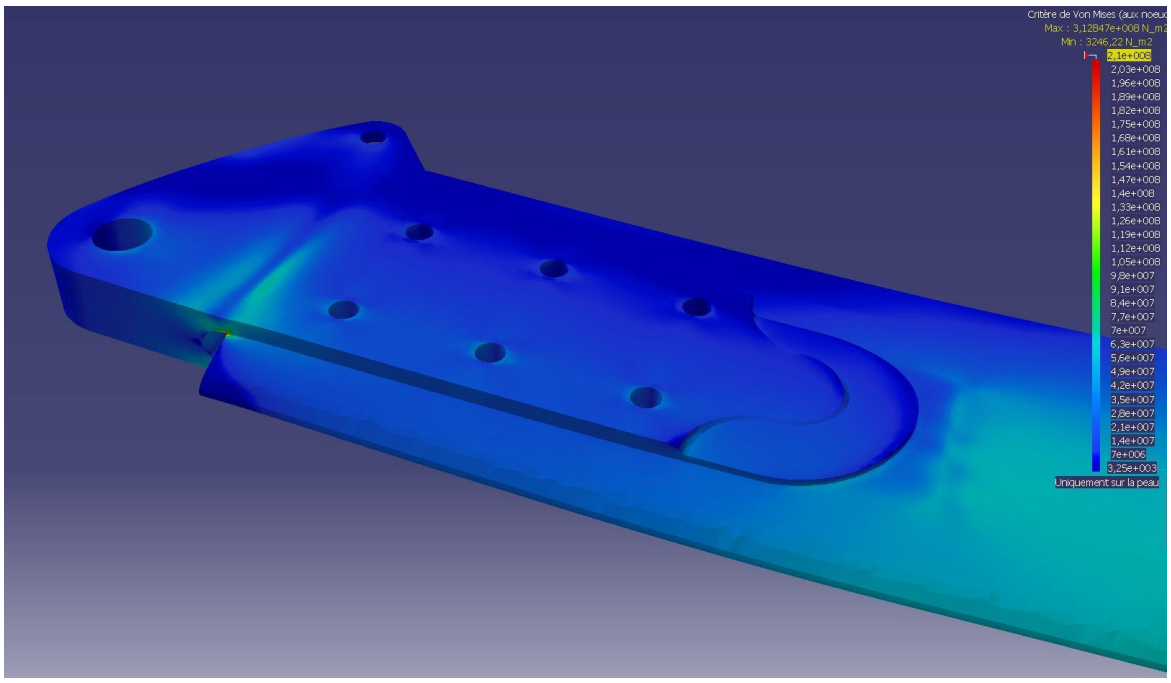

Figure 4: FEA of blade retention plates.
The effect of epoxy filling can be seen at the right end of the retention plate.

The t/k issue:

Equivalent Hover Time t/k is the time that the stored kinetic energy could supply the power required to hover before stalling.

The polar moment of inertia of 2 rotors, constituted by *b* blades is:

$$I_0 \approx b.\int_0^R m'.r^2.\ dr\ = b.m'.\frac{R}{0}\left[\frac{1}{3}.\ r^3\right] + C, \qquad where\ m' = \frac{Mt}{b\ .R} \qquad => I_0 = \frac{Mt}{3}.R^2$$

For b=4, a total mass of blades, $Mt = 4\ .1.9 = 7.6\ Kg$, and an average rotor radius R= 2.32 m, it comes: $I_0 =$ 13.63 $m^2.Kg$

$with\ \Omega = \frac{\pi.N}{30} = 78.5\ rad/sec$ (at 750 RPM)

For a hover requiring 41 Hp, the t/k ratio becomes :

$$\frac{t}{k} = \frac{I_0.\Omega^2}{4\ .\ P\ .750} = \frac{13.63\ .\ 78.5^2}{4\ .\ 41\ .750} = \ 0.68\ sec$$

Although the helicopter is unable to autorotate, this machine exhibits a t/k factor that violates all common "*best practice*" guidelines. However, it has to be put in the context of a demonstrator designed *to hover, and/or fly close to the ground*, and this drawback was accepted in view of the substantial weight saving achieved by removing the swashplates, and control linkages.

Torque balance, at maximum thrust (310 kg lift, at 616 Amps) was obtained at 2.0 degree and 4.9 degrees of pitch, on the upper rotor and lower rotor respectively, at 1000' AMSL, and 23 Deg C OAT.

Ground resonance was a concern during the initial design phase. As both rotors may rotate at slightly different speeds, producing low frequency beating transmitted through the gimbal assembly, that it might drive the airframe into ground resonance. This constraint drove the design of the landing gear, and a highly dissipative structure presenting a flat response over a broad range of frequency was employed. Furthermore, oscillations of the gimbaled front end are damped by dissipative bungees. This has proven to be very light an effective solution (using high hysteresis rubber compounds). Ground resonance analysis was performed using Deutsch and Coleman methods.

In practice, each rotor was separately brought to 0.1 IPS by precise adjustment of the lag links, and tracking. Then only, could both rotors be run together. No ground resonance was ever experienced.

Drive train:

The entire machine's design revolves around the power train (ref 7). Considerable effort was spent on efficiency analysis. The take-off weight is 247 Kg, with an empty weight of 170 Kg. 32 KW, distributed over two DC motors is necessary to hover out of ground effect at 1000 feet AMSL, in ISA conditions.
Brushed motors were employed due to their excellent performance, both in torque and efficiency (91.5%) (ref 24), along with ease of integration (no optical encoders, Hall Effect sensors etc…), (ref 8, 9, 10, 11, 30). Controllers for DC motors are simple, reliable, yet very efficient. However, the required power is on the high side of what can be achieved with conventional brushed motor technologies.

Custom made MOSFET (appendix-symbols) controllers offering 98.5 % efficiency were used (Rds on < 2.5 mΩ), with no need for a heavy cooling system. The drawback of such a solution is the relatively low operating voltage of such semiconductors, requiring higher currents, hence heavier bus bars (ref 6); however, those feather light controllers (1.7 Kg for 20 KW continuous) offered significant weight saving (9 Kg), compared to an IGBT (appendix-symbols)/brushless solution (ref 17) and the resulting drive train's weight budget is remarkably good (despite the modest 2 KW/kg of Lynch motors).

Unlike IGBT devices, MOSFETs offer extremely short switching time as well as high transition frequencies. They can operate at high switching frequency; as a result, light weight magnetic circuits based on high permittivity ferrites (toroids) can be used. However EMI/EMC is an issue, as those controllers generate intense high order harmonics up to several hundred

MHz. Electromagnetic shielding (ref 21) of surrounding electronics was a challenge to successfully reject both conducted and radiated interferences, especially due to the fact that power cables could not be shielded, due to weight constraints.

Unlike some hybrid cars, the helicopter's drive train does not use any DC/DC converter in between the battery pack and the motor controller to maintain a constant power on the shaft. Instead, the battery pack is used in the plateau area of the discharge curve, just post initial sag. Substantial weight saving, and efficiency improvement can be achieved, but only 80% of the battery's capacity can be used this way.

Speed reduction was achieved through high performance carbon fiber synchronous belts. End to end drive train efficiency from battery terminals to rotors shafts is 87.5%.

Battery pack:

The Rechargeable Energy Storage System (RESS) is designed around KOKAM Li-ion polymer pouch cells, offering 160 Wh/Kg, and using a sophisticated battery management system supplied by LiTHIUM BALANCE, Denmark (ref 1, 18, 29). Sourcing and qualifying cells offering the needed flat discharge pattern was a real challenge in itself. Innovative methods and materials were used to combine mechanical protection of large and fragile pouch cells, as well as cooling. A combination of conduction and convection cooling based on aluminum honeycomb heat sinking structure enabled the RESS to deliver 43 KW continuous and 52 KW peak for 10 seconds. The tricky thermal instability of lithium/cobalt chemistry does not leave room for error, and advanced thermal and electrical analysis had to be conducted (Figure 5a and 5b). Battery bank design and thermal analysis represented a substantial part of the whole project time.

If put in short circuit (in case of a crash for example), Li-ion polymer batteries can deliver extremely high peaks of currents that will vaporize small conductors, or induce battery thermal runaway if the short is of a heavier gage (eg: airframe). To avoid this danger, common sense dictates to distribute fuses along the chain of cells. However, due to the high currents involved (620 Amps max), fuse's weight was unacceptably high (1.5 Kg per fuse), so it was decided to trade safety for weight.
Slivers plated bus bars, analyzed using Melson & Both relations (ref 1) were shaped in such way to be part of the cooling circuit (ref 5, 6, 27). The most drastic temperature rises of large pouch cells when discharged at high current for short duration occur in the terminal area where current density is the highest. If not properly cooled, localized aging can occur hence reducing cell capacity.

It is important to note that the cells themselves are not a danger; KOKAM nail-tests all their products and they are proven to be safe, but the particular assembly of cells is making the pack less safe due to absence of fuses. In case of a crash, the possible short circuits could be catastrophic.
An Aerogel based firewall was used between the battery bank and the seat. This material offers outstanding fire resistance combined to unparalleled lightness. Battery frame was made of aluminum honeycomb panels (Figure 6).

In practice, a ground based cooling system cools the pack during the charging period and brings the temperature down to 15 to 20 °C before takeoff. Thermal inertia contributes to 40% of temperature limitations during the flight. Dry ice - fan combination can be used, but was never necessary.

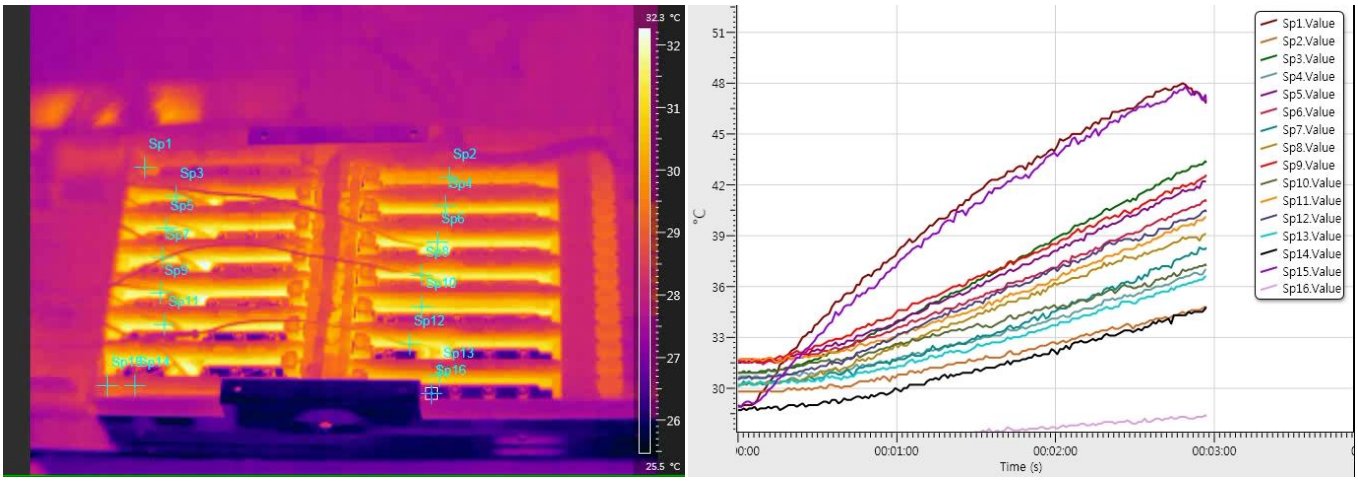

Figure 5a: Thermal analysis of bus bars and battery pack.

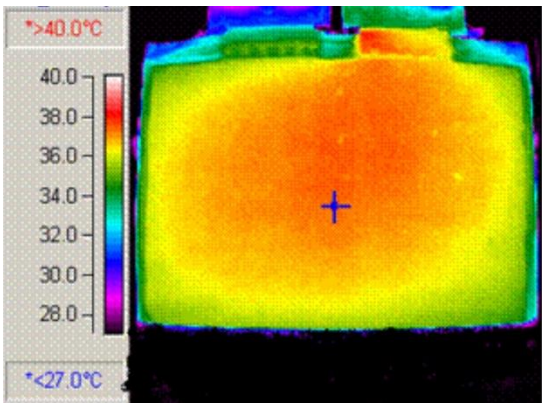

Figure 5-b: Thermal measurement of one cell.

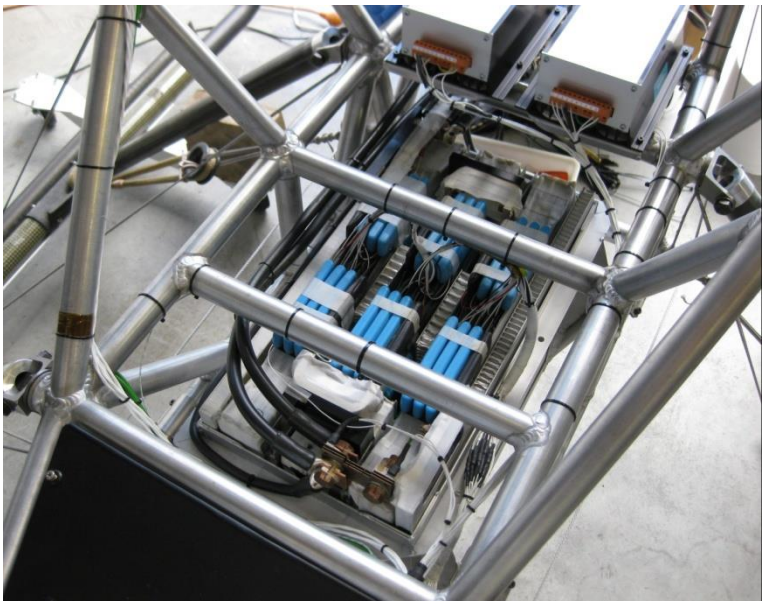

Figure 6: Mechanical arrangement of the pack.

Flight controls:

New solutions had to be found to drastically reduce the weight of conventional flight controls.
Roll and pitch are achieved through a gimbaled front end. Yaw control is achieved through a combination of electric controls in the form of resolvers linked to the yaw pedals and acting on the controllers (Figure 7, right), as well as mechanical linkage acting on a tail fin that intercepts the rotors' downwash. The tail fin produces instantaneous yaw response by deflecting rotor downwash. As for yaw, collective pitch is an electrical control, in form of a flat wheel located on the control stick (Figure 7, left).

Electrical flight control management was achieved by a triple redundant Op-Amp based processor (ref 16, 28). Going analog instead of using a common microcontroller may appear as a Stone-Age choice, but it was a deliberate decision made to speed up development, and prevent possible crashes subsequent to program glitches. Digital flight control systems take a lot of time to be fully tested as programming faults can lie in the software for a long time before being detected. Detecting programming faults at system level is even more time consuming.

Once fine-tuned, (all gains and time constant adjusted), our analog processor proved to be extremely resilient to electromagnetic interference and worked flawlessly. The development, construction, and integration took less than two weeks.

Figure 7: "Collective" (power) control on the left, and yaw controls on the right.

Stress and fatigue analysis:

As the machine is a demonstrator, all main components are calculated for a 700-hour service life only. Every single component was subjected to finite element analysis on CATIA V5R16, and subsequent fatigue Figures were derived. Most calculation methods conform to FAR-27, and MIL-HDBK-5H recommendations (ref 5).

The airframe and energy absorbing landing gear were designed to withstand a 2 m drop and were proven to be very effective during the initial flight tests.

Towards hybrid helicopter

It is very unlikely that current battery technology will make manned electric helicopter viable in the near future, however hybrid architectures can be designed and produced today. Going hybrid significantly increases safety as it replaces all heavy and complex components such as gears, shafts and bearings by highly reliable and redundant semiconductors, copper, and electromagnetic systems. The problem of autorotation is solved once and for all, through the use of high performance batteries.
Up to 40% emissions reduction can be achieved, and hybrid topology prepares the migration towards bio fuels and hydrogen through the integration of highly efficient generator solutions such as aeronautical-grade fuel cells that may become available in the near future. Hybrid propulsion should maintain operator's profit, in a difficult economical context where oil is bound to reach USD 200/ barrel in the future, according to 2010's IEA's forecast.

Safety issues:

Study TM–2000-209597 (table 1), conducted by NASA, covering 8,436 crashes over a 34 years period has shown that 28.5 % of crashes are caused by engine failure, whilst 12.8 % of crashes are caused by internal component / airframe failures, over which a significant part goes to transmission failure (main rotor gearbox, and tail rotor gearbox, transmission shafts, flex plates etc…).

Loss of engine power	2,408 (28.5%)
In-flight collision with object	1,322 (15.7%)
Loss of control	1,114 (13.2%)
Airframe/component/system failure or malfunction	1,083 (12.8%)
Other first event categories	2,509 (29.7%)
Total	**8,436**

Table 1: NASA TM–2000-209597 study results.

Regulatory bodies tend to impose the use of twin engine for urban operations, as well as for numerous missions. Civil Aviation Regulations only address engine failure, but do not solve transmission failure, and the operating cost of a twin engine machine is roughly 1.5 to twice the cost of a single engine, with a negative impact on operator's profitability. As a result the number of small operators plummeted over the last few years. Besides, One Engine Inoperative (OEI) Emergency can be poorly managed by the pilot, and has been responsible for crashes.

System design:

Looking at system level (Figure 8), critical areas follow a closely interlinked tetrahedral pattern:

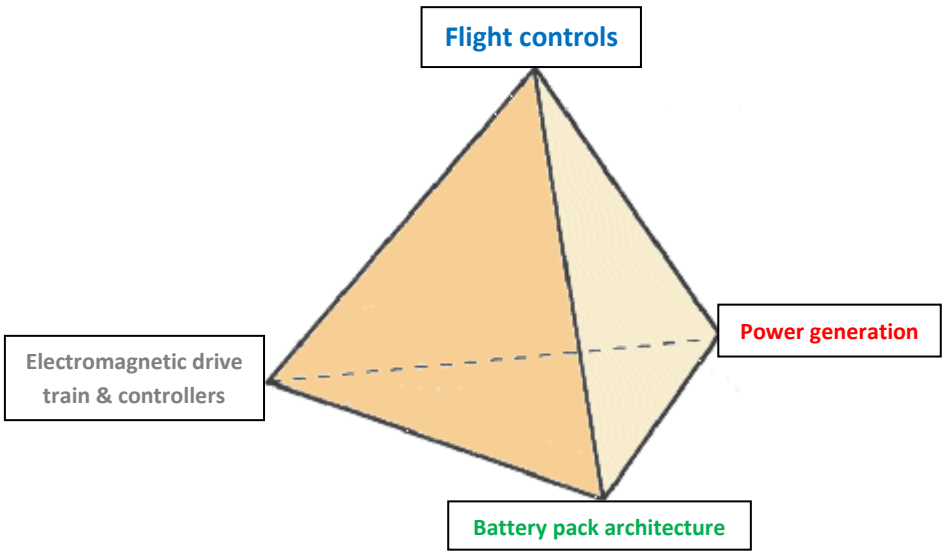

Figure 8: Areas of development

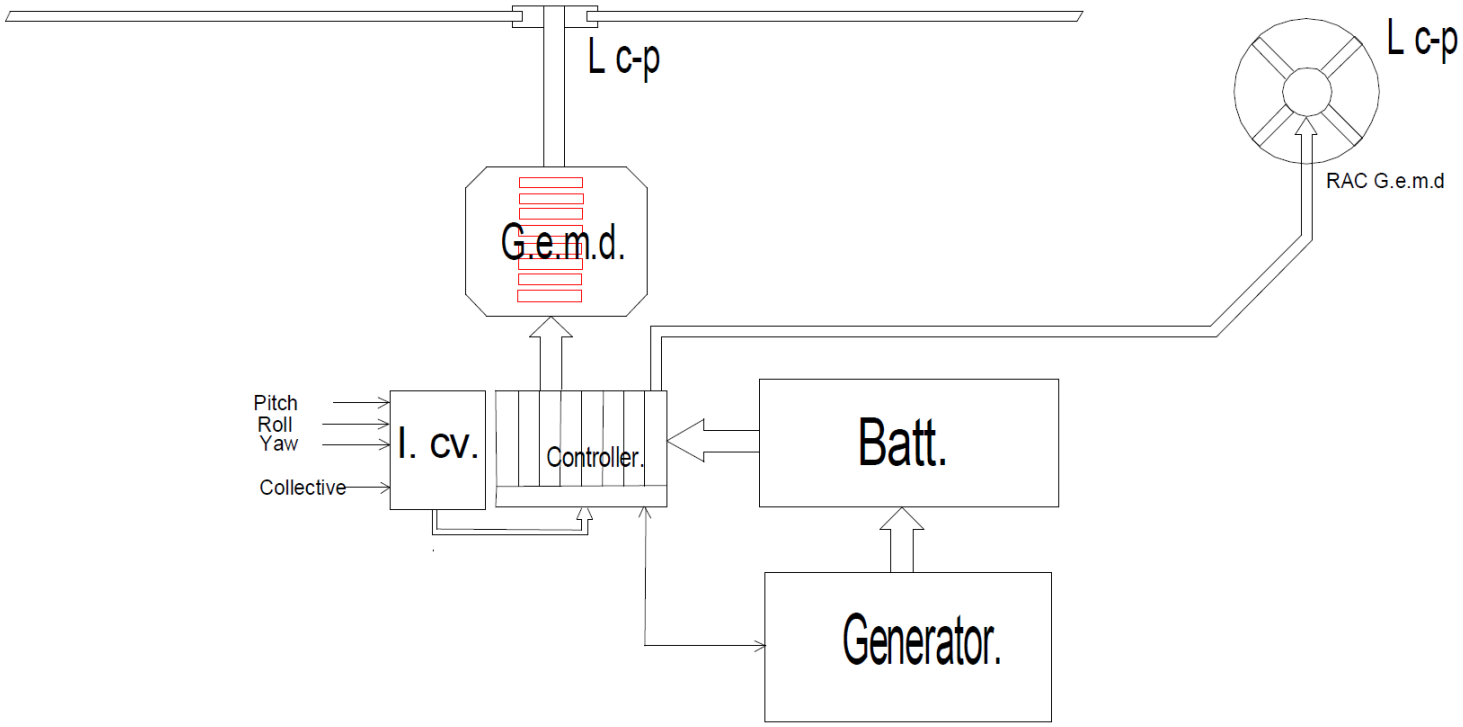

Figure 9: typical arrangement of a series hybrid configuration.

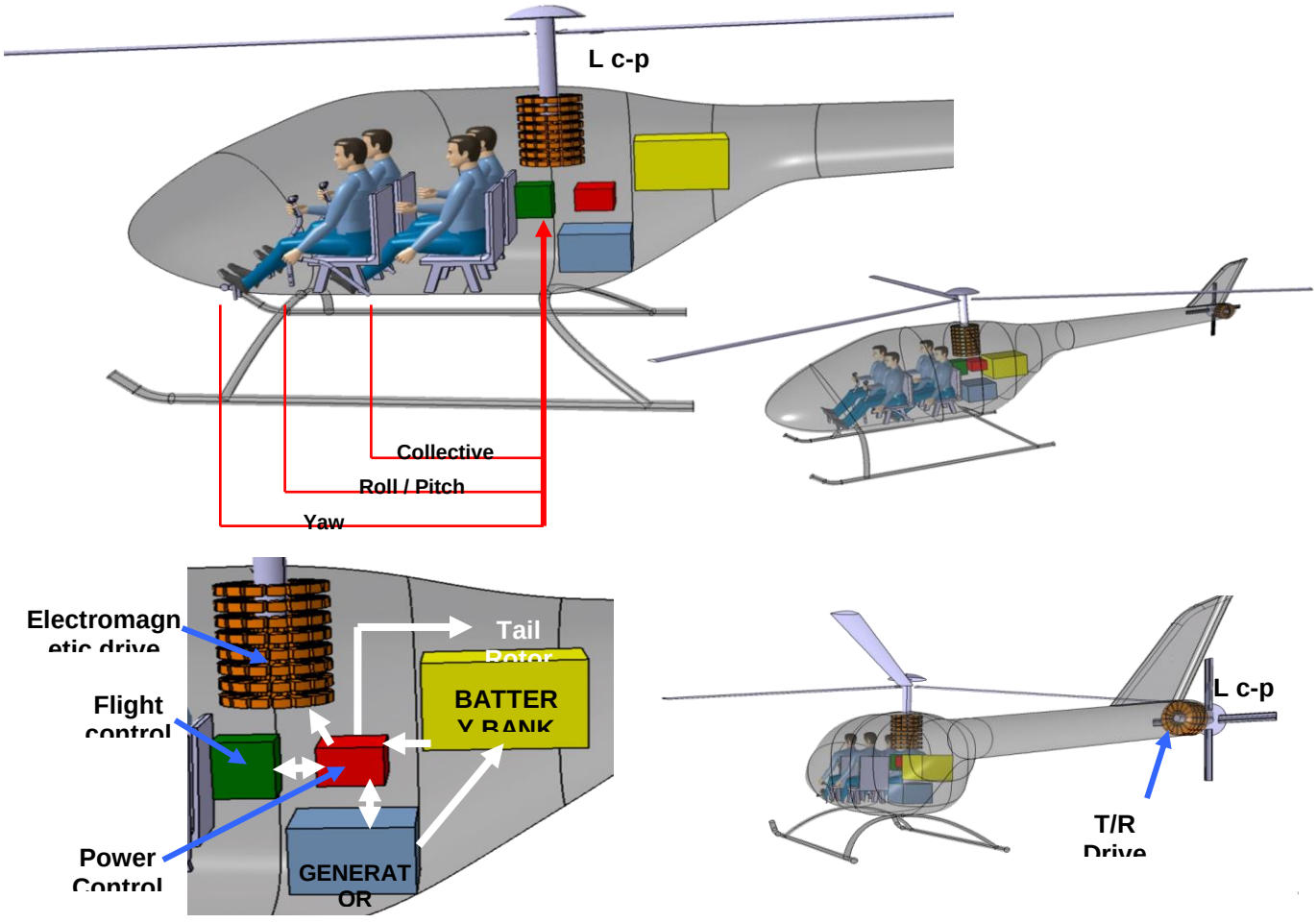

Figure 10: Typical direct drive arrangement.

Figure 9 and 10 depict the typical arrangement of a direct drive hybrid system:

A generator: fuel cell, internal combustion engine, etc… produces electrical power that is stored in the battery bank as well as used by the electromagnetic transmission, through the controller. To be thermodynamically efficient, a piston driven generator is more desirable than a turbine. However, rotation is not necessary and a lighter system such as a two stroke Diesel linear free piston engine is a desirable option. Up to 18% weight saving can be achieved by removing the crankshaft.
The electromagnetic transmission can be roughly described as a highly redundant group of integrated direct drive motors, distributed in **ɵ** (angular), as well as in **z** (height), and organized in a self-healing configuration and referred as GEMD (Annex-Symbols). This transmission includes multiple power circuits and associated circuitry, electromagnetic freewheeling units as well as a multitude of vital devices for cooling, health monitoring, optical fiber interface, and power management. For a given shaft power, there is only one optimum number of elements, that offers the best power to weight ratio, and this is depending on the type of magnetic layout (axial flux, radial flux, variable reluctance), as well as the mechanical design. This particular arrangement is now covered by three patents.

Flight control interface is now connected to the power controller unit, as the end design no longer use conventional swashplates, thanks to a proprietary pitch control system.

The Battery pack calls for a specific design, since conventional planar configuration such as what is used on the demonstrator is definitely not the proper way to achieve safe, reliable, and well cooled systems. A new structural architecture under patent will allow for easy maintenance, a high level of redundancy, and yet will keep copper weight to the bare minimum.

None of those components are available *on the shelf*, and trying to build a prototype with stock parts will only result in an impractical craft.

Technical and operational advantages:

The transmission is a highly redundant system, resilient to single point of failures and ballistic impact, unlike a conventional gearbox. For instance, the overall system reliability of 4 parallel motor elements, each one offering 95% reliability over a 10,000 hours period is 99.999375 %. A single generator drive train could replace conventional twin engine machines in urban operations at the running cost of a single engine helicopter, whereas a twin generator arrangement would be necessary for offshore operations. Paralleling two electrical generators is far easier and more reliable than mechanically combining two turbines into a twin pack.
By storing 2 to 4 minutes of flying time in the battery pack, autorotation is not an issue anymore. The, generator failure has no immediate effect on the flight, and for the pilot, the emergency is far easier to manage than on a twin engine machine. The dead man curve (height/velocity diagram) is almost wiped out, resulting in improved take off profile in urban areas.

The tail rotor is a scale model of the main transmission. Unlike conventional helicopters, there is no longer a fixed ratio between main rotor RPM and tail rotor RPM. This allows for improved flexibility and safety, in sling work operation for instance where tail rotor speed can be slightly increased, to alleviate blade stall, Loss of Tail rotor Effectiveness etc…
Tail rotor speed can be reduced during cruise to save on profile power.

There is no need for an oversized turbine able to produce, roughly 130% power during 5 min at take off: a hybrid system combines the energy stored in the batteries with the energy produced by the generator, as depicted in Annex 3. Unlike mechanical gearboxes which have constant reduction ratio, it is now possible to decrease the main rotor RPM in cruise for additional fuel savings, and yet keeping the generator at its most efficient operating point.

Lastly, the generator can be shut down on demand for short “cold” flight to drastically lower infrared signature.

Weight consideration:

Preliminary design, analysis and simulation for a 1200 Kg MTOW machine are summarized in table 2:

	Conventional helicopter	Hybrid Helicopter
Mass	Kg	Kg
Continental engine IO-550 derated to 180 KW	230	
transmission + freewheeling + tail shaft/bearings + clutch	55	
170 KW Generator		130
Electromagnetic transmission		47
Controller		26
Batteries (11.3 KWH; 450V; 15C cont / 18C peak)		80
Total	285	283

Table 2: Weight budget comparison.

It comes clear that there is no weight advantage in going hybrid; however, energy savings and safety are increased by a magnitude.

The present configuration using 80 Kg of Li Po battery offers:

- 126 KW during 2 min (descent), then 180 KW during 1 minute (landing with hover), **or**, 2nd case :
- 180 KW during 2.4 minutes.

It is worth noting that the batteries will discharge at 15C (that is 15 times its rated Capacity), with peaks up to 18C. Only a specific layout will allow safe operation and cooling. Detailed Figures are found in Annex 2.

Technological risk:

Figure 11 summarizes the technological risk:

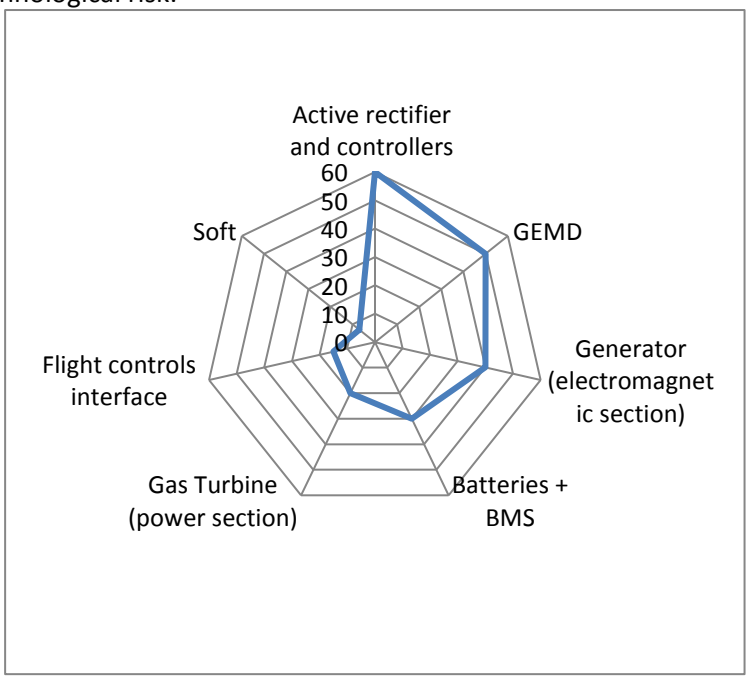

Figure 11: Technological risk

Conclusion:

This unorthodox single-seater helicopter designed, built, and flown in less than a year enabled to make manned flights

close to the ground, and produced very useful data on electrical flight (Figure 12). This craft can be “recycled” into a flying test bed to validate hybrid components.
Hybrid helicopters are at our door step, provided that specific technologies are combined in the appropriate manner. Taken separately, none of the required technologies are exotic to the point that they would make the end goal unrealistic. The emergence of new battery chemistries other than Lithium, and/or fuel cells is making this change of paradigm more real than ever.

Statistically, the rate of fatal accident per million of flight hours is 0.6 in airlines, versus 23 in helicopter aerial work.
We trust that hybrid technologies have the potential to significantly reduce the fatal rate, and this is the driving force to develop those technologies. Fuel savings and reduced operating costs are only a byproduct.

Figure 12: World’s first free flight on the 12th of August 2011.

Annex 1: Specifications of Solution F's demonstrator

- Empty Weight : 170 Kg
- TOGW: 245 Kg
- Max flight duration: 10 minutes

Figure 13: Electric Helicopter.

Construction:

- Aluminum tubing air frame 7020
- Carbon/Kevlar landing gear that can withstand a 2 m drop
- Polyester filament winding is used on the extensible member
- Airframe is designed to withstand 10 G vertical accelerations
- 4130 reinforcement tubing and grade 5 titanium plates are used on hard points
- Total airframe weight: 17 Kg

Propulsion :

- Two 20 KW permanent magnet brushed Agni motors, each one driving one rotor
- Operating voltage: 67 to 72 volts
- IGE total current: 450 to 520 Amps
- Overall transmission efficiency (from battery terminals to rotor shafts): 87.5 %
- Motor controller: high efficiency MOSFET, air cooled. 1.7 Kg per controller
- Transmission reduction ratio: 5.74

Energy :

- Twenty one 106 AH Li Po cells. Power density: 160 WH/Kg
- Nominal voltage: 87 V
- Battery pack weight: 58 Kg including protection casing and passive cooling system
- Battery management system: **LiTHIUM BALANCE**, adapted to our application
- Thermal design, and bus bar system offer an available power of 43 KW continuous, and 52 KW peak (<20 seconds)

Rotor system:

- Two teetering rotors ; 4.74 m diameter (top), and 4.54 m diameter (lower)
- Rotor spacing factor H/D: 0.13
- Tip speed: 180 m/sec in hover IGE
- Airfoils: 8H12; 120 mm chord
- Blade Construction : Multi cells, 6063 T6 alloy
- Conning: 2.21 degrees
- Lag Sweep: + 0.846 Degree

Flight controls:

- Roll/pitch: weight shifting via gimbaled assembly, controlled by an overhead stick
- Yaw : Electrical flight controls acting on differential torque, and tail fin (Instantaneous yaw response, is provided by the tail fin)
- « Collective » (power) : electrical flight controls

Calculation methods / Standards:

- FEA: Dassault CATIA V5R16
- Dynamic stability MSC ADAMS
- Fatigue: MIL-HDBK-5
- Structure, transmission: FAR 27
- EMI/EMC: MIL-STD 461C/462

Annex 2: Preliminary battery sizing for a 1200 Kg hypothetical hybrid helicopter

Hypothetical helicopter specifications:

MTOW :	1200 Kg.
Rotor Diameter :	10.6 m. (Disk area = 88.20 m²)
Blade chord:	0.29 m.
Twist :	-11°.
Hypothetical Airfoil :	NACA 0012.
Tip speed, U :	210 m/sec.
Blade area, Sp :	2.9 m².

Induced power:

Induced velocity:

$$V_i = \sqrt{\frac{F_n}{2.\rho'.S}}$$

Where :

The rotor thrust, F_n= 1200 Kg ;

The air density $\rho' = 0.1225\ Kg\ /\ m^3 (by\ simplifying\ with\ g \approx 10)\ \ at\ Z = 0\ m$,

And the rotor disk area, S=$\frac{\pi D^2}{4}$ = 88.20 m²

$$\boldsymbol{V_i = 7.45\ m/sec}$$

Induced power:

The following empirical approximation that takes into consideration fuselage interaction can be used:

$$P_i = 1.15.m.g.\sqrt{\frac{1}{2.\rho_0}}.\sqrt{\frac{m.g}{S}}\ /745 = 1.15\ .1200\ .\ 9.81.\sqrt{\frac{1}{2\ .\ 1.225}}.\sqrt{\frac{1200\ .\ 9.81}{88.2}}\ /745 =\ 134\ HP$$

Profile power :

For one blade, at a distance r, and with a rotor radius R, it becomes:

$$\frac{F_n}{b} = \frac{1}{2}.C_{zm}.\rho.\int_0^R \Omega^2 .r^2.l.dr = \frac{1}{2}.C_{zm}.l.\rho.\Omega^2.R^3.\int_0^1 \varphi^2.d\varphi$$

Where : b (number of blades) = 2 ; l = Blade chord; U= tip speed = $\Omega.R$, $\varphi = \frac{r}{R}$, and C_{zm} is the average lift coefficient

After integration and by introducing the number of blades, b, it becomes:

$$C_{zm} = \frac{6\,.Fn}{\rho.b.l.R.U^2}$$

In practice, and taking into consideration and tip losses, it becomes:

$$C_{zm} = \frac{6.8\,.Fn}{\rho.b.l.R.U^2}$$

Drag coefficient can be expressed as:

$$C_{xp} = C_{x0} + 0.009.C_{zm}^2$$

For a NACA 0012 we have:

$$C_{xp} = 0.0085.(1 + 1.059{C_{zm}}^2)$$

The torque resulting from profile drag can be expressed as:

$$C = \frac{1}{2}.\rho.C_{xp}.b.l.\Omega^2.\int_0^R r^3.dr = \frac{\rho}{8}.C_{xp}.b.l.U^2.R^2$$

The Passive power can be expressed as: $P_{p0} = C.\Omega = \frac{\rho}{8}.C_{xp}.b.l.R.U^3,$ since $\Omega = \frac{U}{R}$

$$C_{zm} = \frac{6.8.Fn}{\rho.b.l.R.U^2} = \frac{6.8\,.\ 1200\,.\ 9.81}{1.225\,.\ 3.074\,.\ 210^2} = 0.482$$

Note: U= 210 m/s

$$C_{xp} = 0.0085.\left(1 + 1.059{C_{zm}}^2\right) = 0.0085.(1 + 1.059\,.0.482^2) = \ 1.06.\ 10^{-2}$$

$$P_{p0} = C.\Omega = (\frac{\rho}{8}.C_{xp}.b.l.R.U^3)/75 = \ (\frac{0.1225}{8}.1.06.\ 10^{-2}\,.\ 3.074\,.210^3)/75 = \ 61.56HP$$

Required power on rotor shaft: 134 + 61.6 = **195.6 HP**

Total power required : 196 / 0.90 = 218 Hp, or 162 KW (10% losses in tail rotor, and cooling).

Required DC power :

Assuming 90% transmission efficiency, the DC input power will be 180 KW in hover and about 126 KW in economical flight / shallow descent, at 65KT.

Power diagram:

Let's assume two different scenarios of 3 minutes each, distributed as follows:

- 126 KW during 2 min, then 180 KW during 1 minute; that is an average power of 144 KW.
- 180 KW during 2.4 minutes, then 0 KW thereafter.

Let's assume a 450 V pack, and a controller efficiency of 90%;

I = (144,000/450) /0.9 = 355 Amps ≈ 360 Amps.
Q= IT= 360x(1/20) = 18 AH

Assuming that the battery is discharged at 75% (considering an emergency), it comes:
C= 18/0.75= 24 AH ≈25 AH;
The battery is discharged at 360/25= 14.4 C, that is 15C average, (and 18 C peak).
Such discharge preclude planar pack layout, and only a specifically designed architecture such as mentioned in page 11 will fit the bill. At the moment, Li Polymer seems to be one of the very few suitable chemistry.

Battery pack weight:

25AH x 450 V = **11,250 WH**

With the appropriated configuration a pack presenting 140 WH/Kg is achievable, that is a final weight of 11,250/140 = 80 Kg.

Note: As an example, Figures 14 down below summarizes cell availability and pack weight, for the electric demonstrator; Pouch cells offer an unquestionable weight advantage over cylindrical cells such as Gaia, or A123:

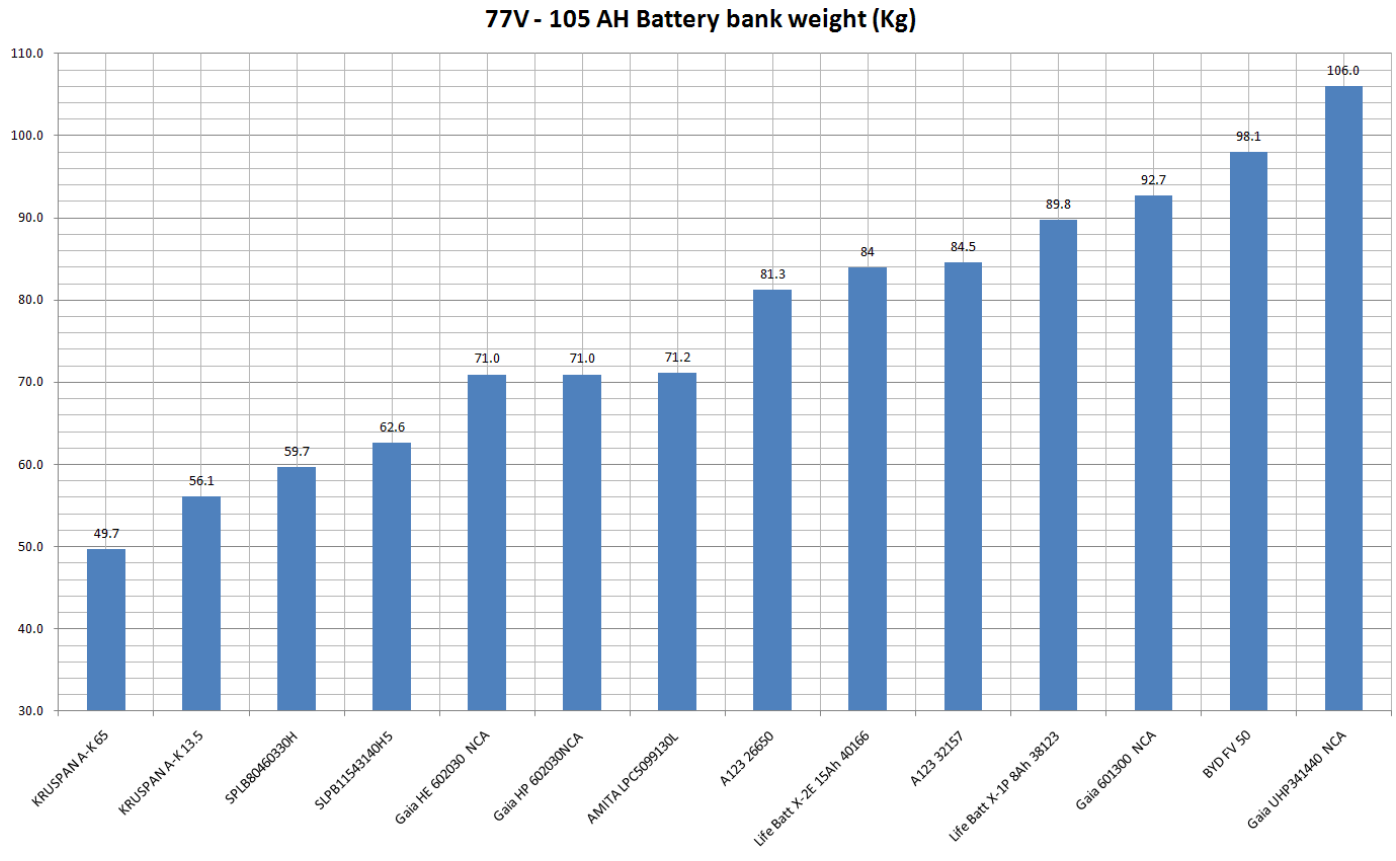

Figure 14: Cell availability and pack weight for the electric demonstrator

Annex 3: Power combination domains:

Figure 15 below is a hybrid system combining the energy stored in the batteries with the energy produced by the generator, during hover, and forward flight.

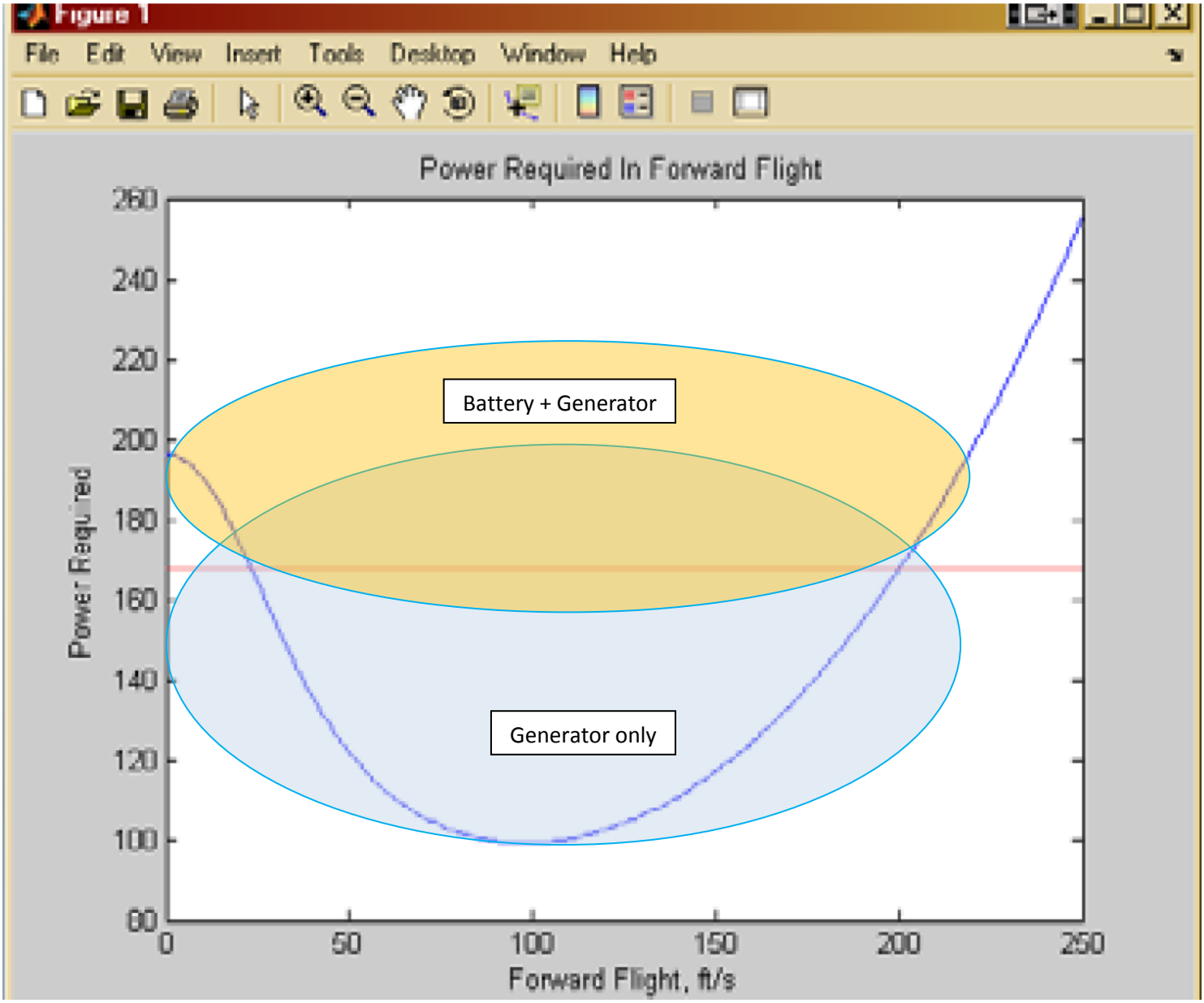

Figure 15: Example of hypothetical helicopter in hover and forward flight.

Acknowledgement:

The author gratefully acknowledges contributions of Doctor Wayne Johnson from the Aeromechanics Branch, NASA Ames Research Center; Doctor Ray Prouty, Professor Richard Brown, from Centre for Future Air-Space Transportation Technology, Glasgow for their review of our initial power calculations; and Tunji Adebusuyi from LiTHIUM BALANCE for his review of our battery system, and his highly valuable expertise.

Appendix—Symbols:

AGL	Above Ground Level
AMSL	Above Mean Sea Level
dB	Decibel
C	Centigrade
CFD	Computational fluid dynamics
CG	Center of gravity
C_L	Lift Coefficient
C_μ	Thrust Coefficient
EMI	ElectroMagnetic Interference.
EMC	ElectroMagnetic Compatibility
FEA	Finite Element Analysis
FAR	Federal Air Regulations
GEMD	Distributed Electromagnetic Drive
Hz	Hertz
IGBT	Insulated Gate Bipolar Transistor
IPS	Inch Per Second
IR	Infrared
LiPo	Lithium Polymer
L/D	Lift to Drag ratio
MOSFET	Metal Oxide Semiconductor Field Effect Transistor
MTOW	Maximum Take-Off Weight
OAT	Outside Air Temperature
Op Amp	Operational Amplifier
Rds on	Drain-Source resistance in “ON” state.
TOGW	Take-Off Gross Weight

References:

Coaxial rotor Power modeling and analysis:

1- Brown L. 1994. Cost-Effective Manufacturing: Joining of Copper and Copper Alloys. In: *CDA Publication No 98*; Published by the Copper Development Association.

2- Brown, R. E. 2009. A Comparison of Coaxial and Conventional Rotor Performance. In: *JOURNAL OF THE AMERICAN HELICOPTER SOCIETY 55*. Alexandria. VA. USA.

3- Brown, R.E. 2008. Modeling the aerodynamics of coaxial helicopters - from an isolated rotor to a complete aircraft. In: *EKC 2008 - Proceedings of the EU-Korea Conference on Science & Technology*. Springer Proceedings in Physics, 124 (XII). Springer Verlag, Germany, pp. 45-59.

4- Coleman, CP. 1997. A Survey of Theoretical and Experimental Coaxial Rotor Aerodynamic Research. In: *NASA Technical Paper 3675.* NASA Ames Research Center, Moffett Field, California. USA.

5- Copper Development Association. 1998. High Conductivity Coppers For Electrical Engineering. In: *CDA Publication No 122*; Published by the Copper Development Association.

6- Copper Development Association. 1997. Electrical Energy Efficiency. In: *CDA Publication No 116*; Published by the Copper Development Association.

7- Dhameja S. 2001. ELECTRIC VEHICLE BATTERY SYSTEMS. Published at Butterworth-Heinemann. Burlington, MA. USA.

8- Emadi, A. 2005. ENERGY-EFFICIENT ELECTRIC MOTORS. Published by Marcel Dekker. New York. USA.

9- Hanselman, D. 2003. Brushless Permanent Magnet Motor Design. Published by Magna Physics Publishing, Lebanon, OH. USA.

10- Jacek F. Gieras. 2002. Permanent magnet motor technology. Published by Marcel Dekker. New York. USA.

11- JACEK F. GIERAS, RONG-JIE WANG, MAARTEN J. KAMPER. 2008. Axial Flux Permanent magnet brushless machines. Published by Kluwer Academic Publishers, Dordrecht. The Netherlands.

12- Johnson, W. 2009. Influence of Lift Offset on Rotorcraft Performance. NASA Ames Research Center, Moffett Field, California. USA.

13- Johnson, W. 1994. Helicopter theory. Courier Dover Publications. Princeton, NJ. USA.

14- Johnson, W. 2009. Hover Performance Correlation for Full-Scale and Model-Scale Coaxial Rotors. In: *JOURNAL OF THE AMERICAN HELICOPTER SOCIETY 54*. Alexandria. VA. USA.

15- Johnson, W. 2009. Design and Analysis of Rotorcraft; In: *NASA/TP–2009-215402*; NDARC NASA. USA.

16- Jung W. 2006. Op Amp Applications Handbook.

17- Khanna V.K. 2003. The Insulated Gate Bipolar Transistor IGBT Theory and Design. Published by IEEE press. Wiley and Son. Hoboken. NJ. USA.

18- KIEHNE. H. A. 2003. BATTERY TECHNOLOGY HANDBOOK. Published by Marcel Dekker. New York. USA.

19- Leishman J.G. 2008. Figure of Merit Definition for Coaxial Rotors. In: *JOURNAL OF THE AMERICAN HELICOPTER SOCIETY*. Alexandria. VA. USA.

20- Leishman J.G. 2006. AERODYNAMIC OPTIMIZATION OF A COAXIAL PROPROTOR. In: *JOURNAL OF THE AMERICAN HELICOPTER SOCIETY*. Alexandria. VA. USA.

21- LOVAT G. 2008. Electromagnetic Shielding. Published by John Wiley & Sons, Inc., Hoboken, New Jersey. USA.

22- MIL-HDBK-17-4. 2002. COMPOSITE MATERIALS HANDBOOK VOLUME 4. METAL MATRIX COMPOSITES. *Department Of Defense publications*. USA.

23- MIL-HDBK-5H. 1998. METALLIC MATERIALS AND ELEMENTS FOR AEROSPACE VEHICLE STRUCTURES. *Department Of Defense publications*. USA.

24- Parviainen A. 2005. DESIGN OF AXIAL-FLUX PERMANENT-MAGNET LOW-SPEED MACHINES AND PERFORMANCE COMPARISON BETWEEN RADIAL-FLUX AND AXIAL-FLUX MACHINES. Thesis presented at Lappeenranta University of Technology. Lappeenranta. Finland.

25- Prouty, R. 1995. Helicopter performance, stability, and control. Krieger Pub; USA.

26- Quinry, J.A.C. 2001. Design Data for Composites. In: *FGI Publication*. Australia.

27- Schoft S. 2001. Joint Resistance of Busbar-Joints with Randomly Rough Surfaces. In: *Proceedings of the 21th Conference on Electrical Contacts 2002, Zurich, pp. 230 – 237.*

28- Terrell D.L. 1996. OP AMPS Design, Application, and Troubleshooting. Published by Butterworth-Heinemann / Elsevier Science (USA).

29- Vincent C. A. 1997. Modern batteries; an Introduction to Electrochemical Power Sources. Published at Butterworth-Heinemann. Burlington, MA. USA.

30- Yeadon W.H. 2001. HANDBOOK OF SMALL ELECTRIC MOTORS. Published by McGraw-Hill, New York, NY. USA.